Article

Cell Reports

# mTORC1 Controls PNS Myelination along the mTORC1-RXRγ-SREBP-Lipid Biosynthesis Axis in Schwann Cells

## Graphical Abstract

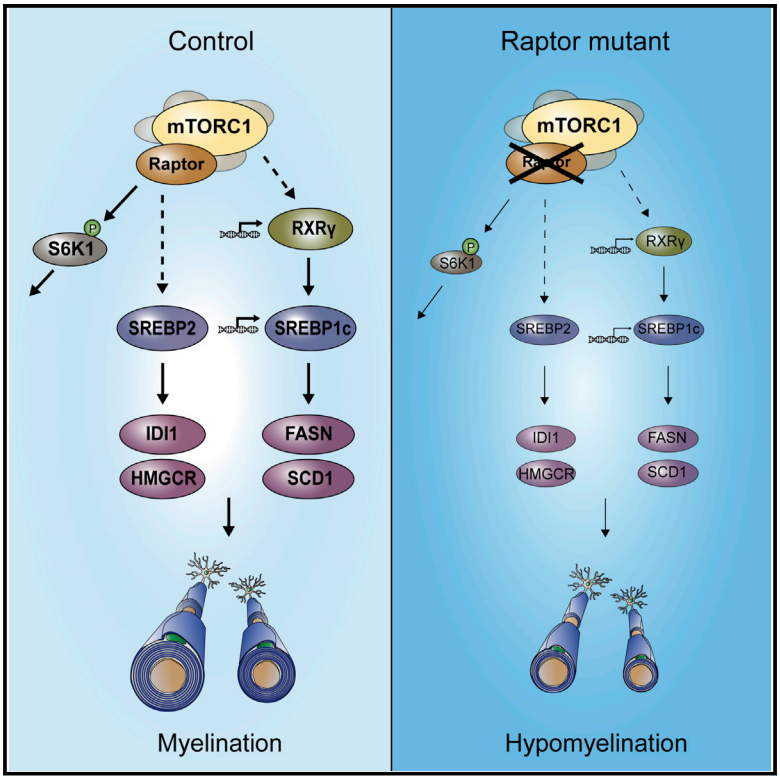


## Highlights

Loss of mTORC1, but not mTORC2, in Schwann cells leads to PNS hypomyelination

Altered lipid composition and decreased nerve conduction accompany the hypomyelination

mTORC1 deficiency causes defective SREBP signaling

In Schwann cells, RXRγ regulates SREBP1c expression downstream of mTORC1

## Authors

Camilla Norrmén, Gianluca Figlia, ..., Michael N. Hall, Ueli Suter

## Correspondence

camilla.norrmen@biol.ethz.ch (C.N.), ueli.suter@biol.ethz.ch (U.S.)

## In Brief

Here, Norrmén et al. identify a central role for the mTORC1 complex in peripheral nerve myelination and provide evidence that SREBPs are key effectors of mTORC1 in regulating Schwann cell lipid biogenesis. They establish the nuclear receptor RXRγ as a downstream target of mTORC1 signaling and show that RXRγ transcriptionally regulates SREBP1c, thus controlling fatty acid metabolism.

Norrmén et al., 2014, Cell Reports 9, 646–660
October 23, 2014 ©2014 The Authors
http://dx.doi.org/10.1016/j.celrep.2014.09.001

OPEN ACCESS
CellPress

Cell Reports
Article

# mTORC1 Controls PNS Myelination along the mTORC1-RXRγ-SREBP-Lipid Biosynthesis Axis in Schwann Cells

Camilla Norrmén,[1,*] Gianluca Figlia,[1] Frédéric Lebrun-Julien,[1] Jorge A. Pereira,[1] Martin Trötzmüller,[2] Harald C. Köfeler,[2] Ville Rantanen,[3] Carsten Wessig,[4,7] Anne-Lieke F. van Deijk,[5] August B. Smit,[5] Mark H.G. Verheijen,[5] Markus A. Rüegg,[6] Michael N. Hall,[6] and Ueli Suter[1,*]

[1]Institute of Molecular Health Sciences, Department of Biology, Swiss Federal Institute of Technology Zurich, ETH Zürich, CH-8093 Zurich, Switzerland

[2]Core Facility for Mass Spectrometry, Center for Medical Research, Medical University of Graz, 8010 Graz, Austria

[3]Research Programs Unit, Genome-Scale Biology, and Institute of Biomedicine, Biochemistry and Developmental Biology, University of Helsinki, 00014 Helsinki, Finland

[4]Department of Neurology, University of Würzburg, 97080 Würzburg, Germany

[5]Department of Molecular and Cellular Neurobiology, Center for Neurogenomics and Cognitive Research, Neuroscience Campus Amsterdam, VU University, 1081HV Amsterdam, the Netherlands

[6]Biozentrum, University of Basel, 4056 Basel, Switzerland

[7]Present address: Ortenau General Hospital, 77654 Offenburg, Germany

*Correspondence: camilla.norrmen@biol.ethz.ch (C.N.), ueli.suter@biol.ethz.ch (U.S.)

http://dx.doi.org/10.1016/j.celrep.2014.09.001



## SUMMARY

**Myelin formation during peripheral nervous system (PNS) development, and reformation after injury and in disease, requires multiple intrinsic and extrinsic signals. Akt/mTOR signaling has emerged as a major player involved, but the molecular mechanisms and downstream effectors are virtually unknown. Here, we have used Schwann-cell-specific conditional gene ablation of *raptor* and *rictor*, which encode essential components of the mTOR complexes 1 (mTORC1) and 2 (mTORC2), respectively, to demonstrate that mTORC1 controls PNS myelination during development. In this process, mTORC1 regulates lipid biosynthesis via sterol regulatory element-binding proteins (SREBPs). This course of action is mediated by the nuclear receptor RXRγ, which transcriptionally regulates SREBP1c downstream of mTORC1. Absence of mTORC1 causes delayed myelination initiation as well as hypomyelination, together with abnormal lipid composition and decreased nerve conduction velocity. Thus, we have identified the mTORC1-RXRγ-SREBP axis controlling lipid biosynthesis as a major contributor to proper peripheral nerve function.**

## INTRODUCTION

The myelin sheath has evolved to enable rapid saltatory propagation of nerve signals, a crucial feature of the vertebrate nervous system. In the peripheral nervous system (PNS), Schwann cells synthesize myelin consisting of tightly compacted layers of plasma membranes around large caliber axons. The particular functional capabilities of the resulting structure depend mainly on its geometry and the specialized protein and high lipid contents of the myelin. Impairments of the myelinated Schwann cell-axon unit due to gene mutations, altered metabolism, or inflammation are frequent causes of diseases, attesting to the crucial importance of PNS myelination (Dyck and Thomas, 2005).

The development of Schwann cells, from immature cells via the promyelinating state to fully myelinating Schwann cells, requires a multitude of regulatory signals. Many of these steps, including cell differentiation, myelination initiation, and determination of the thickness of the myelin sheath, are controlled by the key regulator neuregulin-1 (NRG1) type III, present on the axonal surface (Newbern and Birchmeier, 2010). Mediated by binding to ErbB2/ErbB3 tyrosine kinase receptors on Schwann cells, NRG1 activates second messenger cascades, most prominently the PI3K/Akt, MAPK, and PLCγ pathways (Nave, 2010; Pereira et al., 2012). PI3K/Akt signaling plays a central role in PNS myelination, because Akt in Schwann cells is required for correct myelin sheath thickness (Cotter et al., 2010). In addition, Schwann cell-specific genetic deletion or expression knockdown of the $PIP_3$ phosphatase PTEN (phosphatase and tensin homolog), a negative regulator of Akt activity, resulted in increased Akt phosphorylation and caused hypermyelination (Cotter et al., 2010; Goebbels et al., 2012). In contrast, overexpression of constitutively active Akt in Schwann cells had no detectable effects on PNS myelination (Flores et al., 2008). Although this apparent discrepancy waits to be fully resolved, the mTOR (mammalian [or also mechanistic] target of rapamycin) pathway has been implicated as a major effector of Akt in myelination control (Norrmén and Suter, 2013). Consistent with this notion, mice lacking the mTOR kinase in Schwann cells have hypomyelinated sciatic nerves (Sherman et al., 2012).

The mTOR pathway is intimately linked with Akt signaling and forms a major signaling hub in most cell types. It integrates intra- and extracellular cues, such as nutrients, growth factors,

and energy, which are necessary for cell growth, proliferation, and metabolism (Cornu et al., 2013; Laplante and Sabatini, 2012). mTOR is the core kinase in two structurally and functionally distinct protein complexes, mTOR complex 1 (mTORC1) and mTORC2. In addition to mTOR, these complexes contain several adaptors, including the highly conserved and functionally essential proteins raptor (in mTORC1) and rictor (in mTORC2). Targets of mTORC1 include S6K1 (ribosomal S6 kinase 1) and 4E-BP1 (eukaryotic initiation factor 4E-binding protein 1), controlling processes such as ribosomal biogenesis and cap-dependent translation. mTORC2 regulates cytoskeletal organization, cell survival and metabolism through phosphorylation and activation of AGC kinases, including Akt, SGK1 (serum and glucocorticoid-regulated kinase 1) and PKC (protein kinase C). Akt, which, in addition to its phosphorylation by mTORC2, is also phosphorylated and activated by PDK1 (3-phosphoinositide dependent protein kinase 1), in turn, activates mTORC1.

Although Akt/mTOR signaling is evidently essential for myelination, the downstream effectors and the underlying molecular mechanisms of this process remain poorly understood. Moreover, because mTOR activity is functionally divided between mTORC1 and mTORC2, previous studies have not distinguished between these different parts of the pathway (Sherman et al., 2012). Thus, we sought to determine the functional roles of the individual mTOR complexes in the regulation of PNS myelination, and to identify contributors to the molecular basis of mTOR-dependent myelination. To this end, we have analyzed the roles of mTORC1 and mTORC2 functions in the developing mouse PNS by conditionally deleting *raptor*, *rictor*, or both together, specifically in Schwann cells. We found that signaling by mTORC1 is critical for PNS myelination, including timely myelination initiation and extent of myelination. Control of lipid synthesis via SREBP transcription factors, including mTORC1-dependent control of SREBP1c gene expression by the nuclear receptor RXR$\gamma$, was identified as a key component in this process.

## RESULTS

### Loss of Raptor, but Not Rictor, Leads to Impaired Initiation, and Extent of Myelination but Does Not Affect Differentiation to Promyelinating Schwann Cells

To study the functions of mTORC1 and mTORC2 during PNS myelination, we generated mouse mutants lacking raptor (mTORC1), or rictor (mTORC2), or both raptor and rictor, in Schwann cells. To this effect, we crossed mice carrying floxed alleles of *raptor* and/or *rictor* (Bentzinger et al., 2008; Polak et al., 2008) with mice expressing Cre-recombinase under control of the Desert hedgehog (*Dhh*) promoter (Jaegle et al., 2003). First, we verified the specific loss of raptor and/or rictor proteins in the corresponding mouse mutants by western blot analysis of sciatic nerve lysates at postnatal day (P) 5 (Figure S1A). Residual amounts of protein are likely from nonrecombined fibroblast and neurons of the nerves. We then assessed morphological consequences in the mutant nerves. Analyses of toluidine-blue-stained semithin cross-sections of P60 sciatic nerves revealed robustly reduced nerve sizes in raptor mutants and raptor/rictor double mutants, compared to control nerves, whereas rictor mutant nerves were indistinguishable from controls (Figure 1A). Closer inspection revealed modest reductions of myelinated axon numbers per nerve and in the area covered by myelinated axons, whereas axon density was increased in raptor and raptor/rictor mutants (Figures 1A and S1B). Evaluations of mean axon diameters uncovered a decrease in raptor and raptor/rictor mutants (Figure 1A), a finding mainly explained by the absence of large caliber axons (above 6 $\mu$m) in these nerves (Figures 1A and 1B). Detailed size distribution analysis did not yield major differences in other size categories, beyond a slight increase in smaller to middle-sized axons in raptor and raptor/rictor mutants (Figure 1A). The most striking feature found, however, was substantial hypomyelination in sciatic nerves of raptor and raptor/rictor mutants, quantitatively confirmed by the determination of g-ratios (ratio of axon diameter divided by fiber diameter) (Figure 1B). Axons of all calibers exhibited thinner myelin sheaths in these mutants, whereas axons of rictor mutants showed normal myelin thickness (Figure 1B). Thinner myelin was already evident in raptor and raptor/rictor mutants at P5, when most Schwann cells had just started to myelinate (Figures 1C and S1C). G-ratio quantifications in raptor mutant and control nerves analyzed over time (P5 to 12 months) revealed the largest difference in myelin at P60, when developmental myelination is essentially complete. Of note, as raptor mutants got older, myelin slowly continued to grow, as indicated by significantly decreased g-ratios at 6 and 12 months of age compared to P60. However, myelin thickness in raptor mutants never reached that of control mice, at least until 12 months of age, the last time point examined. Thus, despite continued myelin growth in raptor mutants, full recovery was not achieved. Hypomyelination in raptor mutants was not restricted to distal nerves, or motor or sensory fibers, because this feature was also evident in both dorsal and ventral roots, containing only sensory or motor fibers, respectively (Figure S1D). Moreover, analysis of teased nerve fibers revealed decreased internodal lengths in raptor mutants (Figure S1E), indicating that loss of raptor affects longitudinal as well as radial Schwann cell growth, consistent with previous findings in mTOR-deficient Schwann cells (Sherman et al., 2012).

During nerve development, immature Schwann cells envelop bundles of axons. Subsequently, these cells single out large caliber axons in a radial sorting process, establishing a 1:1 relationship as promyelinating Schwann cells surrounding individual axons (reviewed in Jessen and Mirsky, 2005). At P5, raptor mutant and littermate control nerves had a similar number of promyelinating Schwann cells (Figure 2A, yellow arrowheads), consistent with equal staining for the promyelinating marker Oct6 (Figure 2B) and equal Oct6 protein levels determined by western blotting (Figure 2C). These results indicate that differentiation from immature to promyelinating Schwann cells is not majorly affected in raptor mutant nerves. However, at P14, when all promyelinating Schwann cells in control or rictor mutant nerves had started to myelinate, raptor and raptor/rictor mutant nerves still contained high numbers of Schwann cells left in a promyelinating state (Figures 2A and 2B and S2A), indicating a delay in the onset of myelination. At P60, the transition block from the promyelinating to myelinating state had been overcome, because highly Oct6-expressing cells or 1:1 relationships were no longer present (data not shown).

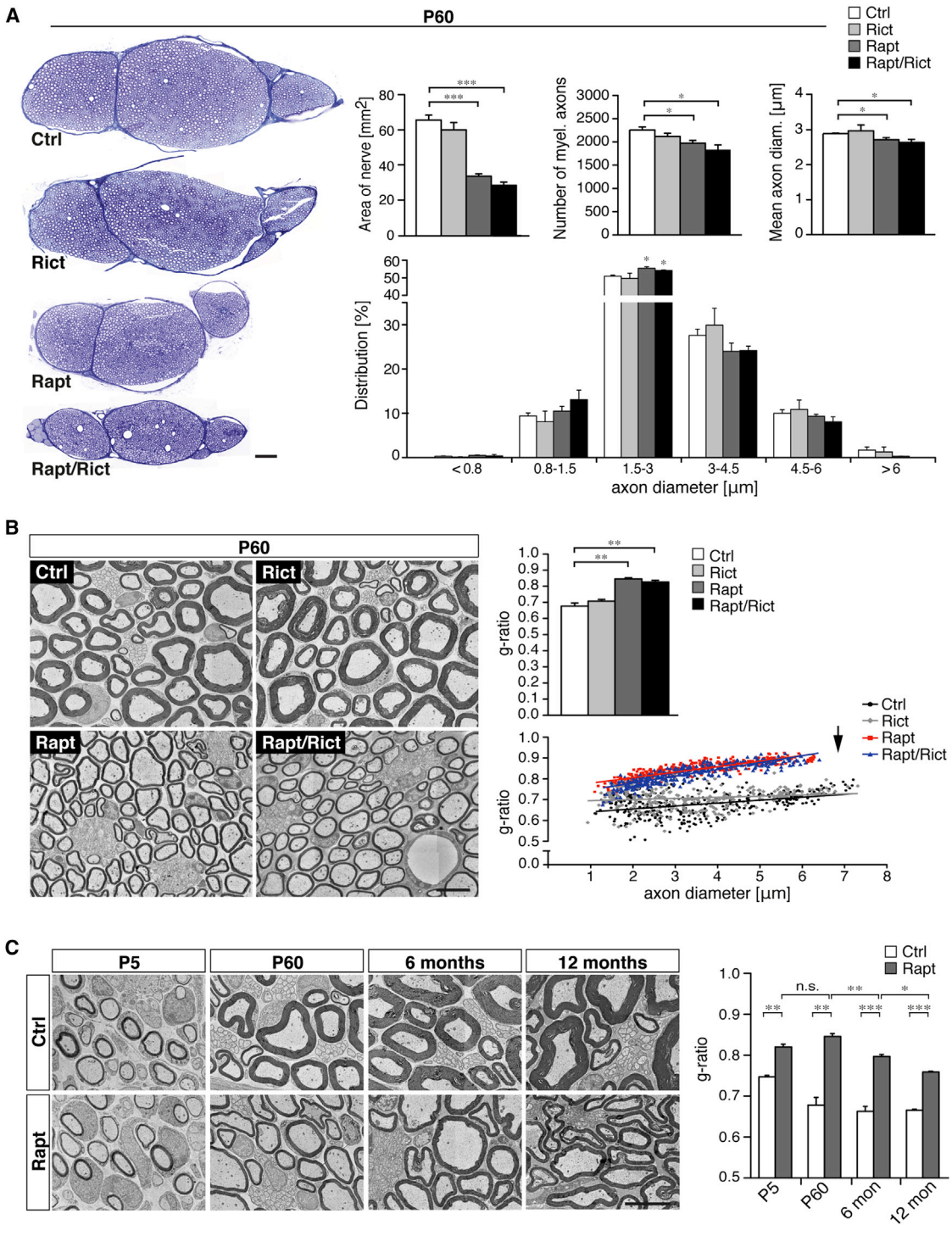


**Figure 1. PNS Hypomyelination in Mouse Nerves Lacking Raptor in Schwann Cells**

(A) Toluidine-blue-stained semithin sections of sciatic nerves from control (Ctrl), rictor (Rict), raptor (Rapt), and raptor/rictor (Rapt/Rict) mutant mice at P60, showing smaller nerves in raptor and raptor/rictor mutants. Scale bar, 50 μm. Nerve area, numbers, and mean axon diameter of all myelinated axons in the main fascicle were quantified, showing a significant decrease in nerve area, slightly fewer myelinated axons, and smaller mean axon diameter. Percentual distribution of axon diameters is shown divided in six size classes. Results are the mean from three different mice per genotype. Error bars: SEM. *p < 0.05, ***p < 0.001. (B) EM micrographs of ultrathin cross-sections of sciatic nerves from control, rictor, raptor, and raptor/rictor mutant mice at P60, showing hypomyelination in raptor and raptor/rictor mice. Scale bar, 5 μm. Myelin thickness was quantified as g-ratio (axon diameter divided by fiber diameter) and plotted against the axon

*(legend continued on next page)*

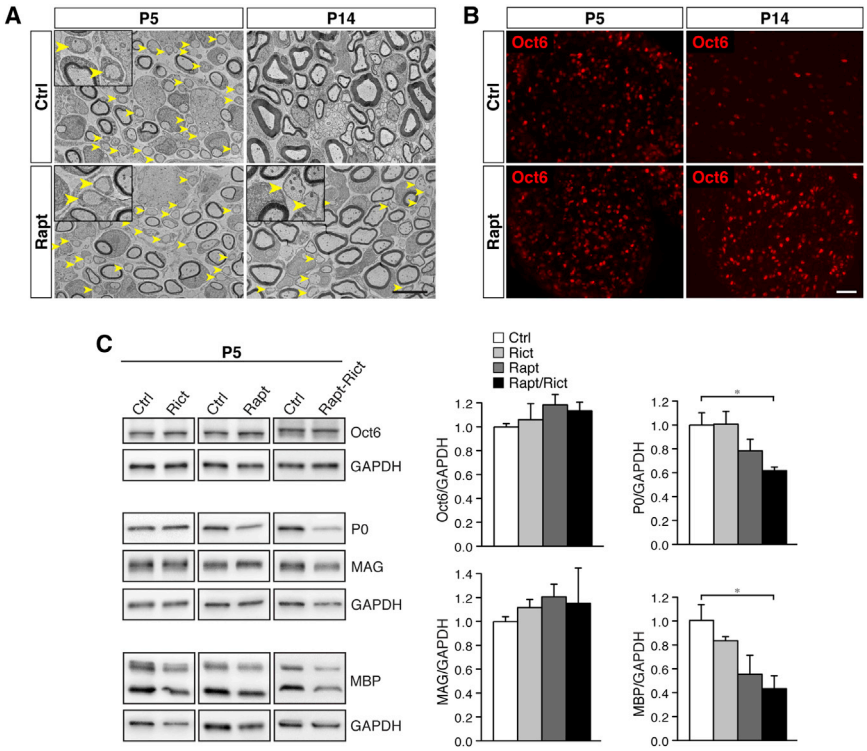


**Figure 2. Loss of Raptor Causes Delayed Onset of Myelination**

(A) EM micrographs of ultrathin cross-sections of sciatic nerves from control and raptor mutant mice at P5 and P14, showing similar numbers of pro-myelinating Schwann cells in a 1:1 relation with axons (yellow arrowheads) in raptor mutants and controls at P5. At P14, there is persistence of 1:1 relations in mutants, whereas in controls all Schwann cells have progressed to a myelinating state (except those in Remak bundles). Insets show examples of 1:1 Schwann cell-axon units. Scale bar, 5 μm.

(B) Oct6 immunostaining of transverse cryosections from control and raptor mutant sciatic nerves at P5 and P14, showing similar numbers of Oct6-expressing cells in raptor mutants and controls at P5, whereas at P14 there is continued high Oct6 expression only in raptor mutants, indicative of a delay in the onset of myelination. Scale bar, 50 μm.

(C) Western blot analysis of myelin proteins in sciatic nerve lysates from control, rictor, raptor, and raptor/rictor mutant mice at P5. Expression levels from at least three mice per genotype were quantified, and average levels are shown relative to control mice. Error bars: SEM. *p < 0.05.

See also Figure S2.

Raptor mutants also showed defects in radial sorting and Remak bundle formation, with large immature bundles still present at P60 (Figure S2B). In controls and rictor mutants all large caliber axons had been sorted out from the maturing bundles prior to P14, leaving only mature Remak bundles associated with nonmyelinating Schwann cells (Figure S2B). In raptor mutants, Remak bundles with regular morphology could not be found even at P60. Instead, the bundles present were abnormally large (although smaller than at P14, see quantification in Figure S2B), containing axons of mixed calibers without Schwann cell cytoplasm between individual axons, similar to previous reports describing radial sorting defects (Pellegatta et al., 2013; Pereira et al., 2009). At 6 months, bundles in raptor mutants were considerably smaller and had taken a more Remak bundle-like structure, where Schwann cell cytoplasm was present around some of the axons (Figure S2B). Analyses of 8-month-old sympathetic trunks with an enrichment of small caliber axons and Remak bundles were in line with the results from sciatic nerves, demonstrating that raptor mutants with time can form Remak bundle-like structures, albeit with fewer axons and abnormal morphology (Figure S2C).

Next, we studied the expression of major myelin proteins and transcription factors in sciatic nerves during active myelination. At P5, MBP and P0 protein levels were modestly reduced in raptor/rictor double mutants compared to controls, with a similar trend also in raptor mutants, whereas MAG was unaltered (Figure 2C). No major changes in protein expression of main transcriptional regulators of the PNS myelination program, Sox10, Krox20, and Oct6, were observed in any mutants at this stage (Figure 2C; data not shown).

Taken together, our data show that raptor/mTORC1 in Schwann cells is a critical regulator of myelination initiation and myelin growth in the PNS. Because these processes were not detectably altered in Schwann cells lacking rictor/mTORC2, we conclude that functional mTOR signaling in developing myelinating Schwann cells is predominantly mediated by mTORC1, similar to recent findings in oligodendrocytes (Bercury et al., 2014; Lebrun-Julien et al., 2014).

## Altered Signaling due to Inactivation of *raptor* or *rictor* Affects Akt Activation

To elucidate signaling pathways affected in nerves of the mutant mice, we analyzed the signaling downstream of mTORC1 and mTORC2. As expected, 4E-BP1 and S6K, common phosphorylation targets of mTORC1, were hypophosphorylated in raptor

diameter. Note the absence of large caliber axons in raptor and raptor/rictor mutants (arrow in g-ratio plot). At least 100 axons per animal were analyzed. n = 3 mice for each genotype. Error bars: SEM. **p < 0.01.

(C) EM micrographs of ultrathin cross-sections of sciatic nerves from control and raptor mutant mice at P5, P60, 6 months, and 12 months of age, showing hypomyelination in raptor mutants already at P5, and lasting at least until 12 months of age. The hypomyelination becomes less severe with age (past P60). Scale bar, 5 μm. Myelin thickness was quantified as the g-ratio. At least 100 axons per animal were analyzed. n = 3 mice for each genotype. Error bars: SEM. *p < 0.05, **p < 0.01, ***p < 0.001.

See also Figure S1.

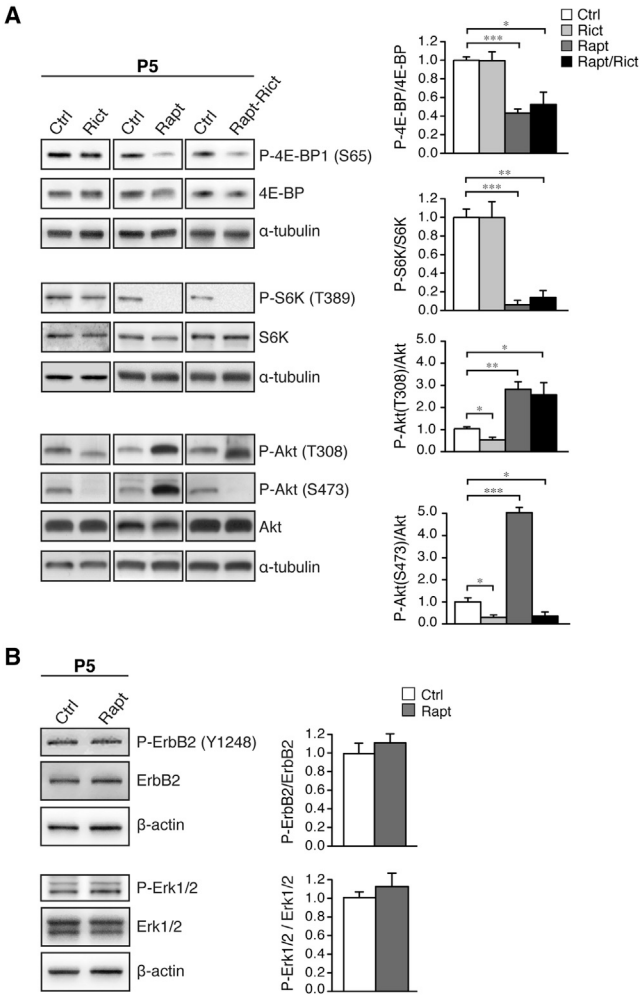


**Figure 3. Decreased mTORC1 Signaling and Increased Akt Phosphorylation in Raptor Mutant Mice**

(A) Western blot analysis of phosphorylation status of mTORC1 and mTORC2 targets in sciatic nerve lysates from control, rictor, raptor, and raptor/rictor mutant mice at P5. Expression levels of at least three mice per genotype were quantified, and average levels are shown relative to control mice. Error bars: SEM. *p < 0.05, **p < 0.01, ***p < 0.001.

(B) Western blot analysis of sciatic nerve lysates from control and raptor mutant mice at P5, showing no significant differences in ErbB2 or Erk1/2 phosphorylation. Expression levels from at least three mice per genotype were quantified, and average levels are shown relative to control mice. Error bars: SEM.

See also Figure S3.

and raptor/rictor mutants, but not in rictor mutants (Figure 3A). Furthermore, P-Akt (T308), which is phosphorylated by PDK1, was strongly hyperphosphorylated in raptor and raptor/rictor mutants (Figure 3A). This finding is likely due to the absence of negative feedback loops that normally act downstream of mTORC1/S6K1 to ensure inhibition of upstream growth factor signaling upon prolonged or excessive mTORC1 activity (Efeyan and Sabatini, 2010). The mTORC2 target P-Akt (S473) was strongly decreased in rictor and raptor/rictor mutants, consistent with the loss of the functionally required mTORC2 component rictor. In raptor mutants, however, P-Akt (S473) was hyperphosphorylated, suggesting that loss of the negative feedback loops downstream of mTORC1/S6K in raptor mutants also affects mTORC2 activity. Of note, the Akt species recognized by anti P-Akt (T308) antibodies migrated slightly faster in SDS gel analysis of sciatic nerve lysates of rictor mutants (and of raptor/rictor mutants) (Figure 3A), consistent with previous observations (Sherman et al., 2012). This finding points to differences in Akt isoforms expressed or, more likely, posttranslational modifications (such as differential phosphorylation of sites other than T308 and S473) in nerves lacking rictor.

Based on the defects observed in Schwann cell myelination in raptor mutants, we looked for alterations in known signaling pathways regulating these processes. We detected no differences in the activation of the ErbB2/ErbB3 receptor complex (P-ErbB2/ErbB2) or the activation of the MAPK pathway at the level of Erk signaling (P-Erk1/2/Erk1/2) (Figure 3B), or in protein levels of PTEN, integrin β1, and ILK in raptor mutants compared to controls (Figure S3).

## Loss of mTORC1 Activity in Schwann Cells Leads to Defective SREBP Signaling

During myelination, the Schwann cell membrane expands several thousand-fold (Webster, 1971), requiring high amounts of lipid biosynthesis. The sterol regulatory element-binding proteins (SREBPs) are transcription factors that regulate expression of the majority of enzymes necessary for fatty acid and cholesterol synthesis, with SREBP1c mainly regulating enzymes of the fatty acid synthesis pathway and SREBP2 primarily cholesterol synthesis enzymes (Shao and Espenshade, 2012). SREBPs are synthesized as inactive full-length precursors bound to SCAP (SREBP cleavage-activating protein) and INSIG (insulin-induced gene) in the endoplasmic reticulum (ER) (Shao and Espenshade, 2012). In a sterol-dependent fashion, the SREBPs are transported to the Golgi for proteolytic processing. Once cleaved, mature SREBPs enter the nucleus to act as transcription factors. mTOR signaling regulates SREBP activity in various cell types in a variety of ways (Bakan and Laplante, 2012; Porstmann et al., 2008). SCAP, in turn, is required for proper PNS myelination (Verheijen et al., 2009). Thus, we analyzed expression of SREBP1 and SREBP2 in mTORC1- and mTORC2-deficient nerves. Indeed, protein levels of full-length SREBP1 were reduced in raptor and raptor/rictor mutants, as were SREBP1c mRNA levels, whereas rictor mutants expressed levels comparable to controls (Figure 4A). Also, the SREBP1 target genes FASN (fatty acid synthase) and SCD1 (stearoyl-CoA desaturase 1) were strongly downregulated in raptor nerves both at the protein and mRNA levels (Figures 4A and 4B), whereas rictor mutant nerves showed protein levels equal to controls. These findings indicate that SREBP1 transcription and activity are decreased in mTORC1-deficient but not mTORC2-deficient nerves. However, neither protein levels of full-length SREBP2 nor SREBP2 transcripts were reduced in raptor mutants, despite that the SREBP2 target proteins HMGCR (3-hydroxy-3-methylglutaryl-CoA reductase) and IDI1 (isopentenyl-diphosphate delta isomerase 1) were strongly downregulated both at the protein and mRNA levels (Figures 4A and 4B). These results indicate that SREBP2 activity

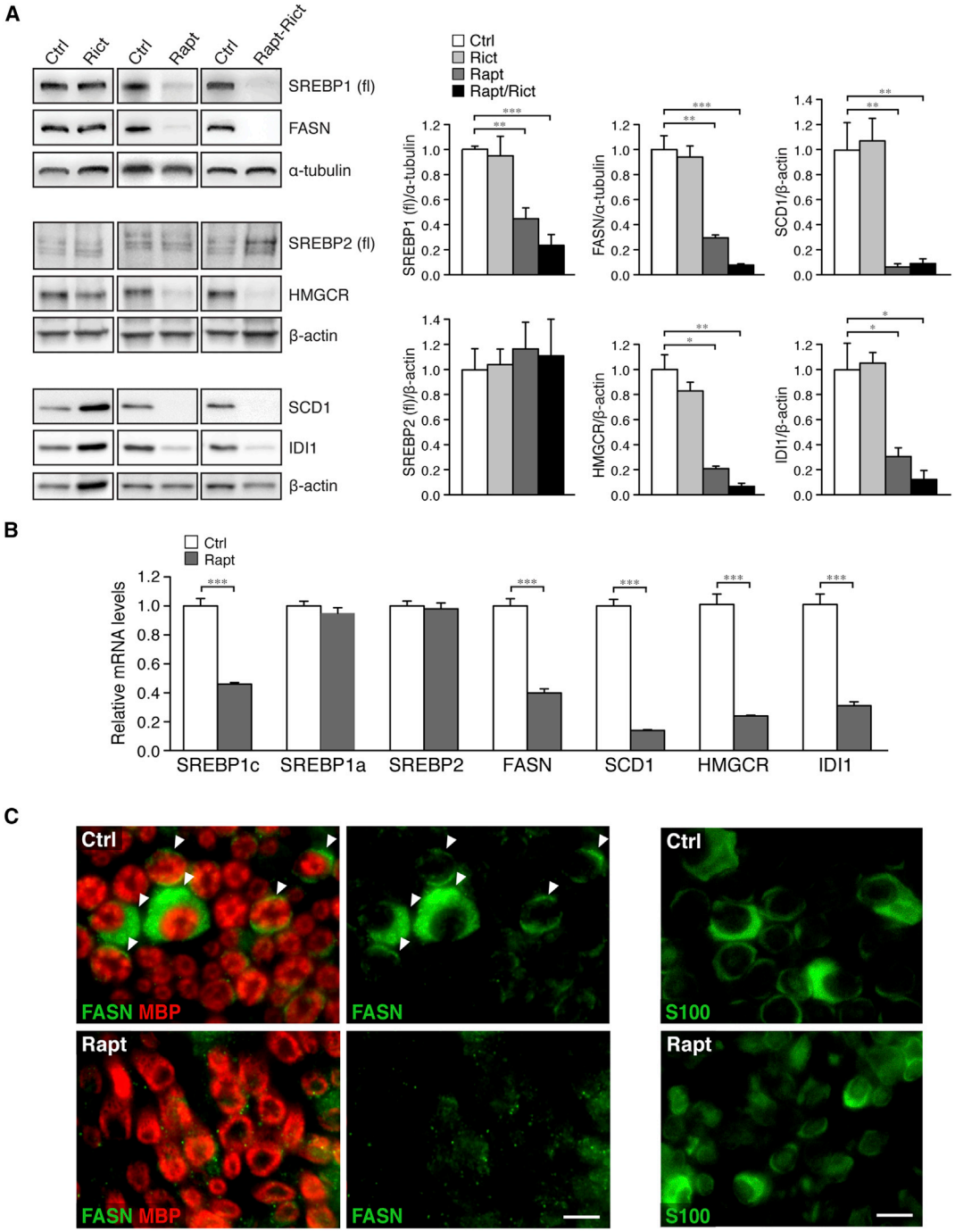


**Figure 4. Deficient mTORC1 Activity Leads to Decreased SREBP Signaling**

(A) Western blot analysis of SREBP proteins and their targets in sciatic nerve lysates from control, rictor, raptor, and raptor/rictor mutant mice at P8, showing decreased full-length SREBP1, FASN, and SCD1 expression. Expression of full-length SREBP2 is not changed, although its targets HMGCR and IDI1 are downregulated. The expression in at least three mice per genotype was quantified and is shown as average values normalized to those in control mice. Error bars: SEM. *$p < 0.05$, **$p < 0.01$, ***$p < 0.001$.

(B) qRT-PCR analysis of SREBPs and their target gene expression in sciatic nerve lysates from control and raptor mutant mice at P8, shown as relative transcript levels compared to controls. The mRNA levels of target genes of SREBP1c and SREBP2 are reduced, as are SREBP1c levels themselves, whereas SREBP1a and SREP2 levels are comparable to those in control mice. n = 4 mice for each genotype. Error bars: SEM. ***$p < 0.001$.

(C) Immunostaining for FASN (green) and the myelin marker MBP (red) in transverse cryosections from control and raptor mutant sciatic nerves at P14, showing loss of FASN in raptor mutant Schwann cell cytoplasm. Immunostaining for the Schwann cell cytoplasm marker S100 (pseudo-colored in green) in separate sections shows that the cytoplasmic compartment of raptor mutant Schwann cells appears normal. Scale bar, 5 μm.

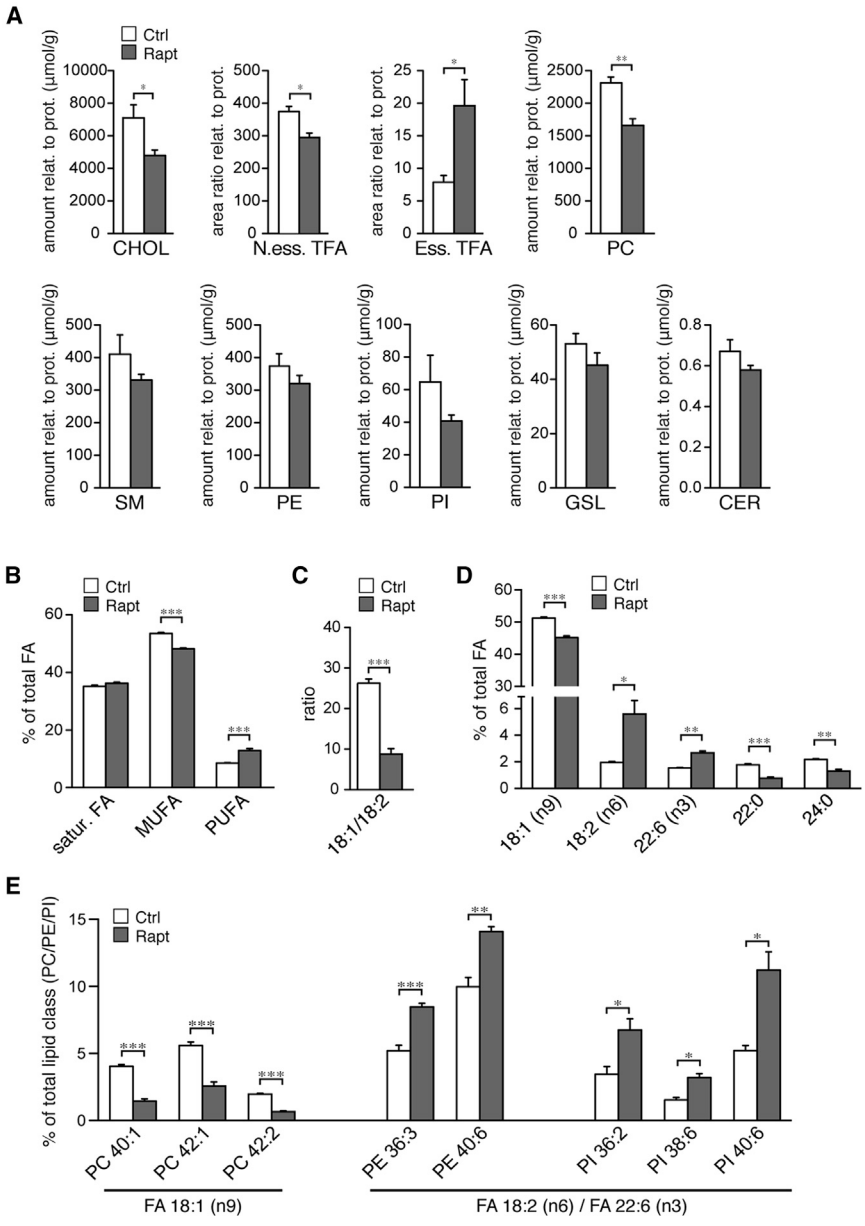


**Figure 5. Abnormal Lipid Composition in Nerves of Raptor Mutant Mice**

Lipid extracts of P60 sciatic nerves from control and raptor mutant mice were analyzed using liquid chromatography-mass spectrometry for nonessential and essential fatty acids (N.ess FA; Ess. FA) and all major lipid classes (CHOL, cholesterol; PC, phosphatidylcholine; PE, phosphatidylethanolamine; PI, phosphatidylinositol; SM, sphingomyelin; CER, ceramide; GSL, glycosylceramide). n = 3 animals for control mice, n = 4 for raptor mutant mice. Error bars: SEM. *p < 0.05, **p < 0.01, ***p < 0.001. See also Figure S4.

(A) Amounts of each lipid class normalized to total protein content.

(B and C) Percentage of saturated fatty acids (FA), monounsaturated FAs (MUFA), and polyunsaturated FAs (PUFA) among total FAs, as well as the ratio between MUFA 18:1 and essential PUFA 18:2, indicating a shift from MUFAs to PUFAs in raptor mutants.

(D) Percentage of indicated FAs compared to total FAs. FA 18:1, the most abundant FA in Schwann cells, as well as myelin enriched very-long-chain fatty acids (VLCFA) 22:0 and 24:0, were significantly downregulated in raptor mutant nerves. Levels of essential and conditionally essential FAs 18:2 and 22:6 were instead significantly increased in raptor mutants.

(E) Examples of individual lipid species containing FAs 18:1, 18:2, or 22:6, showing that changes in raptor mutants for these lipids are similar to those for the FAs they incorporate (shown in D).

See also Figure S4.

is decreased in mTORC1-deficient Schwann cells compared to controls but, unlike SREBP1c, this activity is regulated by post-transcriptional, likely even posttranslational, mechanisms. No changes were found in transcript levels for SREBP1a, a minor SREBP isoform expressed at low levels in Schwann cells (Figure 4B). Finally, we confirmed by immunohistochemistry on cross-sections of sciatic nerves that the loss of the SREBP1 target FASN observed in sciatic nerve lysates in raptor mutants occurred indeed in Schwann cells (Figure 4C).

Collectively, these data demonstrate that loss of raptor/mTORC1 signaling in Schwann cells leads to defective SREBP signaling, resulting in downregulation of both SREBP1c and SREBP2 target genes. The mTORC1 complex regulates SREBP1c at the transcriptional level, whereas SREBP2 activity appears to be regulated posttranslationally.

## Aberrant Lipid Composition and Reduced Nerve Conduction Velocity in Nerves of *raptor*-Deficient Mice

The hypomyelination and substantial downregulation of lipogenic and cholesterogenic enzymes in raptor mutants prompted us to analyze the lipid composition of sciatic nerves of raptor mutants and controls. As expected, we found lower levels of cholesterol and nonessential fatty acids (FAs) in raptor mutant nerves (P60; Figure 5A). Of note, raptor mutants showed an absolute increase of essential FAs, which cannot be synthesized by the body and thus require external uptake (Figures 5A and 5D). Increased uptake of FAs from external sources is a likely explanation for this finding. In addition to cholesterol and nonessential FAs, also the amount of total phosphatidylcholine (PC) was reduced. Other major lipid constituents of PNS myelin, such as sphingomyelin (SM), phosphatidylethanolamine (PE), phosphatidylinositol (PI), glycosylceramide (GSL), and ceramide (CER), showed a tendency to be lower in raptor mutants compared to controls, but without reaching statistical significance. Besides the general absolute reduction in major lipid classes and in several individual lipid species when compared to the protein content of the nerves (Figure S4), also the relative

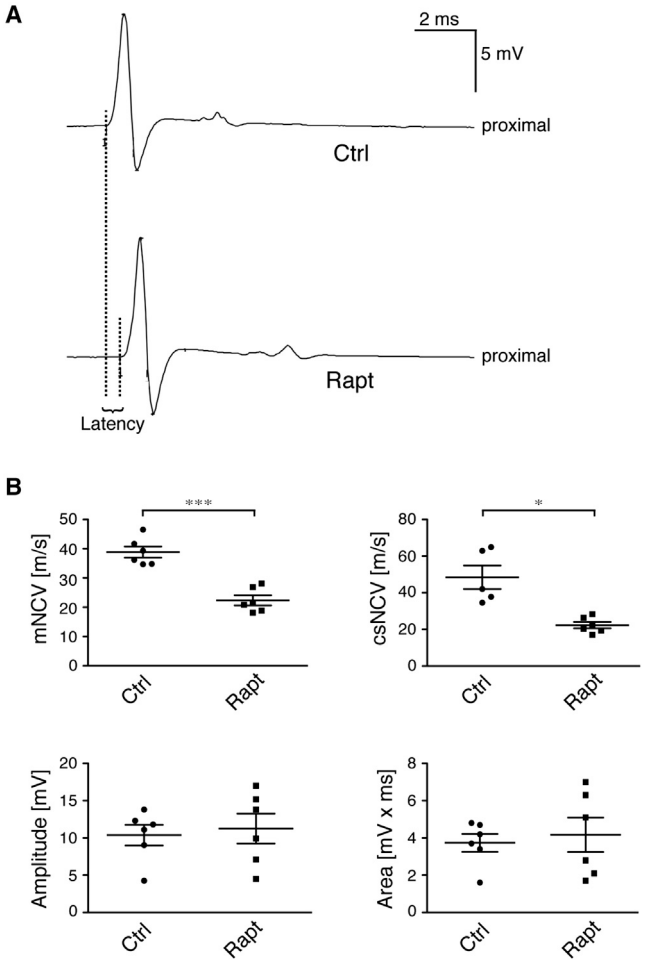


**Figure 6. Reduced Nerve Conduction Velocities in Raptor Mutant Mice**

(A) Representative image of a compound muscle action potential (CMAP) recording (measuring motor nerve conduction velocity, mNVC) from foot muscles after proximal stimulation of sciatic nerves from 4-month-old control and raptor mutant mice. Dotted lines show latency of signals between control and raptor mutant mice.

(B) Vertical scatterplot showing reduction of mNCV, reduction of compound sensory NCV (csNCV), and unchanged amplitude and area of CMAPs in sciatic nerves of raptor mutants. n = 6 mice. mV, millivolt; ms, millisecond; m/s, meter per second. Data are shown as mean ± SEM. *$p < 0.05$, ***$p < 0.001$.

distributions of specific FAs and lipid species were altered in raptor mutants (Figures 5B–5E). There was a shift from monounsaturated fatty acids (MUFAs) toward polyunsaturated fatty acids (PUFA) in raptor mutants (Figure 5B), which was also seen in the decreased ratio of FAs 18:1 (oleic acid) to 18:2 (linoleic acid) (Figure 5C). The nonessential FA 18:1 is the most abundant FA in Schwann cell myelin, whereas FA 18:2 is an essential FA. Thus, the decreased 18:1/18:2 ratio reflects the decreased ability of raptor mutants to synthesis FAs. The proportions of FAs 18:1 and 18:2 change during normal PNS development, reflecting accumulation of myelin and providing an index of the myelination status (Garbay et al., 2000). In line with this notion and with our results, a decreased 18:1/18:2 ratio has also been observed in other hypomyelinated mouse mutants, such as the Charcot-Marie-Tooth disease type 1A (CMT1) mouse model *Trembler* (Garbay et al., 1998), and in the Schwann cell-specific SCAP mutant mouse with defective SREBP signaling (Verheijen et al., 2009). The essential and conditionally essential FAs 18:2 and 22:6 were increased both relative to other FAs and when normalized to protein content (Figures 5D and S4). Compared to membranes from other cell types, myelin is specifically enriched in saturated very-long-chain fatty acids (VLCFAs) (22:0 and 24:0). The levels of these FAs were markedly reduced in raptor mutant sciatic nerves (Figure 5D). Finally, alterations in the levels of specific FAs were also reflected in altered levels of the specific lipid species that incorporate these FAs (Figure 5E).

Myelination of nerves allows saltatory conduction, but correct myelin assembly and composition are imperative for proper nerve conduction velocity (NCV). Because we observed significantly thinner myelin sheaths and shortened internodes in raptor mutants, accompanied by an aberrant myelin lipid composition, we performed NCV studies to examine whether the velocity would be compromised in the mutant nerves. Both motor nerve conduction velocity (mNCV) and compound sensory nerve conduction velocity (csNCV) were reduced in raptor mutants (Figure 6A), indicating that both motor and sensory fibers are affected equally, consistent with our observations that the ventral and dorsal roots are both hypomyelinated. Moreover, neither the compound muscle action potential (CMAP) amplitude nor its area was significantly altered (Figure 6B), indicating that all fibers were affected homogenously and no major axon loss had occurred.

In conclusion, our data show that loss of raptor/mTORC1 in Schwann cells leads to abnormal lipid composition of sciatic nerves. This includes a general decrease in cholesterol, total fatty acids, and phosphatidylcholines, likely as a result of the observed decreases in key enzymes involved in fatty acid and cholesterol synthesis. Furthermore, slowed NCV was found in raptor mutant mice, in agreement with the observed hypomyelination, shorter internodes, and changes in lipid composition, demonstrating that raptor/mTORC1 in Schwann cells is crucial for proper nerve physiology.

## The Nuclear Receptor RXRγ Regulates SREBP1c Downstream of mTORC1

To elucidate how SREBP transcription factors are regulated in Schwann cells, and how mTORC1 may influence this regulation, we sought to analyze the SREBP pathway in more detail. The mTORC1 target S6K has been associated with SREBP regulation downstream of mTORC1 (Düvel et al., 2010). Morphologic analysis of adult sciatic nerves from combined *S6K1/2* knockout mice did not, however, reveal defects in myelin thickness and structure (Figure S5A). Also the subcellular localization of lipin1 has been implicated in mTORC1-dependent regulation of SREBP signaling (Peterson et al., 2011). However, immunohistological staining for lipin1 showed partly nuclear staining in both control and raptor mutant nerves, without major differences (Figure S5B). Next, we analyzed gene expression levels of factors involved in SREBP processing, such as SCAP, INSIG proteins, and S1P and S2P proteases (Figure S5C), but could not find

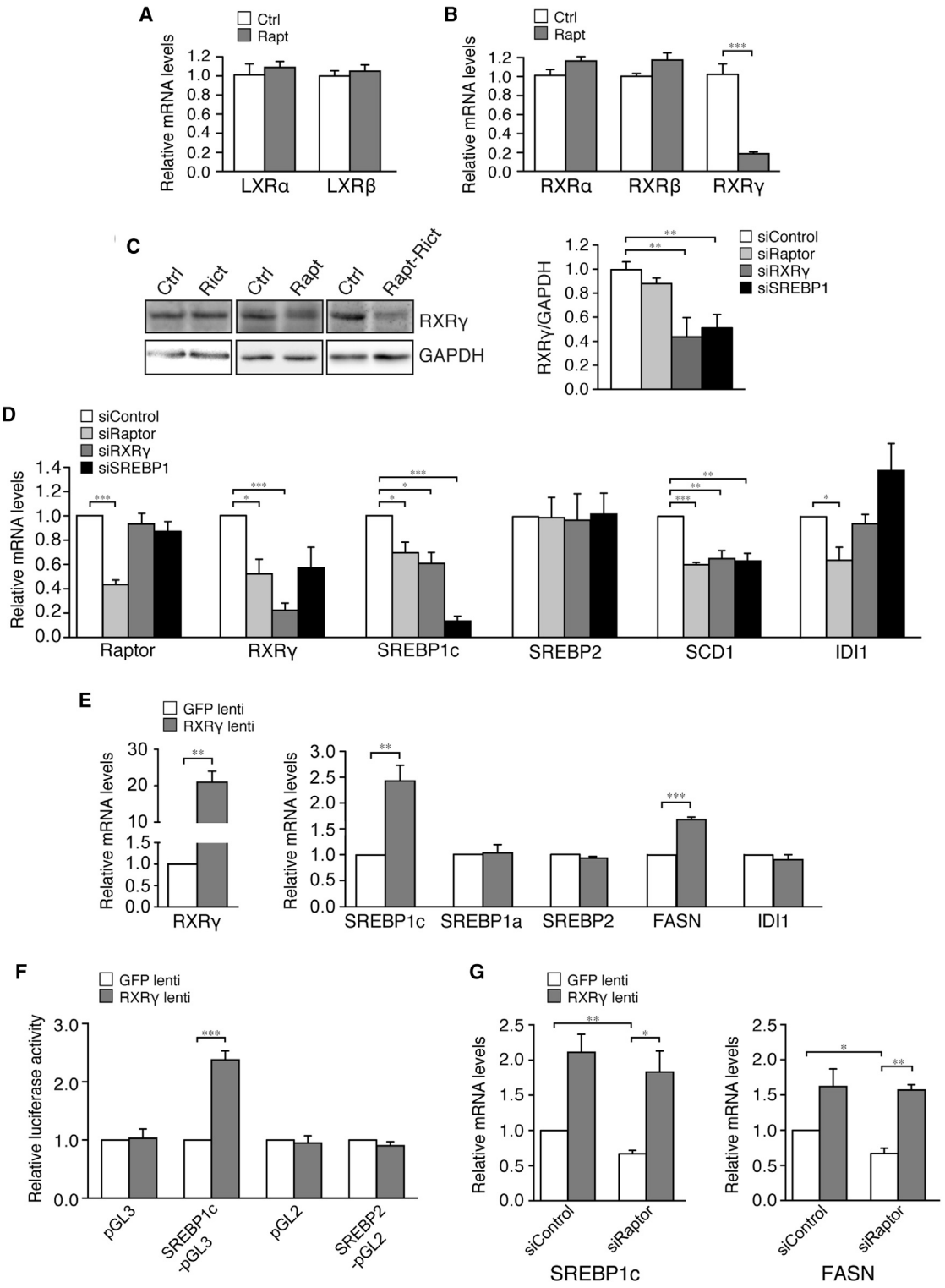


**Figure 7. The Nuclear Receptor RXRγ Regulates SREBP1c Downstream of mTORC1**

(A and B) qRT-PCR analysis expression of liver X and retinoid X nuclear receptors (LXR and RXR) in sciatic nerve lysates from control and raptor mutant mice at P8, shown as mean relative transcript levels compared to controls. Of the nuclear receptors only RXRγ is reduced. n = 4 mice for each genotype. Error bars: SEM. ***p < 0.001.

*(legend continued on next page)*

likely contributors to the decreased SREBP signaling in raptor mutants.

The fact that the mRNA level of SREBP1c was substantially downregulated in raptor mutant nerves (Figure 4B) points to transcriptional regulation as a putative mechanism of how SREBP1c is regulated downstream of mTORC1. SREBP2 activity was also decreased in mTORC1-deficient Schwann cells compared to controls, but, unlike SREBP1c, the mRNA levels were not changed, and hence SREBP2 is not likely regulated transcriptionally by mTORC1. In some cell types, the liver X receptors (LXRs), which are members of the nuclear hormone receptor superfamily, regulate the transcription of *Srebf1c* (encoding SREBP1c) (Repa et al., 2000). We therefore analyzed LXR expression levels in raptor mutant mice. However, mRNA levels of LXRα and LXRβ were not altered compared to controls (Figure 7A). We also analyzed expression levels of the retinoid X receptors (RXRs), a related nuclear receptor family known to heterodimerize with the LXR receptors. Although RXRα and RXRβ transcript levels were unchanged, RXRγ mRNA levels were strongly reduced in raptor mutants (Figure 7B). The amounts of RXRγ were also reduced at the protein level in raptor and raptor/rictor mutants, whereas rictor mutants had RXRγ levels comparable to controls (Figure 7C). Related nuclear receptors of the retinoic acid receptor (RAR) family were not differentially regulated in raptor mutant nerves (Figure S5D) (although RARα showed a tendency for increase), nor were other transcriptional regulators implicated in mTORC1/SREBP signaling, such as YY1 (yin yang 1), PGC-1α (peroxisome proliferator-activated receptor gamma coactivator 1 alpha), and the NF-Y (nuclear transcription factor Y) family (Figures S5E and S5F).

We next turned to cell cultures of primary rat Schwann cells to study the signaling in more detail. In these experiments, knockdown of raptor using small interfering RNA (siRNA) recapitulated at large the observations in raptor mutant mice (Figure 7D). Moreover, when knocking down RXRγ expression, we observed similar downregulation of SREBP1c and its downstream target SCD1 as in raptor mutants in vivo and raptor knockdown in vitro (Figure 7D), suggesting that RXRγ may regulate SREBP1c downstream of mTORC1. Consistent with our findings in raptor mutant nerves, we did not observe changes in SREBP2 transcript levels in raptor or RXRγ knockdown cells. However, whereas raptor knockdown caused downregulation of the SREBP2 target IDI1 similar as in vivo, RXRγ knockdown did not alter IDI1 levels (Figure 7D). Together, these results suggest that, whereas mTORC1 regulates SREBP2 activity in Schwann cells, RXRγ does not regulate SREBP2, but only SREBP1c. To rule out siRNA off-target effects, knockdown experiments were repeated with a second set of siRNAs, yielding similar results (Figure S6A). Next, we overexpressed RXRγ in primary Schwann cells. Consistent with the knockdown results, this treatment led to markedly increased levels of SREBP1c transcripts and its target FASN (Figure 7E), further confirming that RXRγ regulates SREBP1c in Schwann cells. As expected, mRNA levels of SREBP2 and the SREBP2 target IDI1 were not changed (Figure 7E). To confirm that the RXRγ-dependent regulation of SREBP1c was at the transcriptional level, we performed luciferase reporter assays with a reporter construct containing a fragment of the SREBP1c promoter. As expected, RXRγ expression led to activation of the SREBP1c promoter, as seen by increased luciferase activity (Figure 7F), thus indicating regulation of SREBP1c transcription in Schwann cells. The SREBP2 promoter could not be activated by RXRγ overexpression, confirming our results that RXRγ does not regulate SREBP2 signaling. Finally, to demonstrate that the defective SREBP1 signaling in Schwann cells upon raptor deletion is indeed due to decreased RXRγ, we overexpressed RXRγ in Schwann cells with knocked-down expression of raptor. The results show that the decreased levels of SREBP1c and FASN transcripts in raptor knockdown cells could be rescued to similar levels compared to controls by reintroducing higher RXRγ expression (Figures 7G and S6B), corroborating our results that mTORC1 contributes to the control of lipid biosynthesis by RXRγ-dependent transcriptional regulation of SREBP1c.

In conclusion, we have demonstrated that deficient mTORC1 (but not mTORC2) -mediated signaling in Schwann cells leads to hypomyelination, together with an abnormal lipid profile and reduced NCV. Furthermore, we found that SREBP1c and SREBP2 are regulated downstream of mTORC1 in Schwann cells. SREBP1c is regulated transcriptionally, whereas SREBP2 is controlled by other means. Finally, we have established RXRγ as a transcription factor regulated downstream of mTORC1 and shown that RXRγ controls SREBP1c transcription and consequently lipidomic enzyme expression in Schwann cells. Collectively, these data provide a molecular basis for mTORC1-dependent myelin production and underline the importance of mTOR signaling and lipid biosynthesis for correct myelination in the developing PNS.

(C) Western blot analysis showing reduced RXRγ levels in sciatic nerve lysates of raptor and raptor/rictor mutant mice compared to controls at P5. Expression levels in at least three mice per genotype were quantified, and average levels are shown relative to levels from control mice. Error bars: SEM. $^{**}p < 0.01$.

(D) Primary Schwann cells were transfected with a pool of two siRNAs each, or a nontargeting siRNA (siControl), to achieve expression knockdown of raptor, RXRγ, or SREBP1. Expression of indicated genes was analyzed by qRT-PCR, 72 hr posttransfection. Results are shown as mean ratio of siControl levels from three independent experiments. Error bars: SEM. $^{*}p < 0.05$, $^{**}p < 0.01$, $^{***}p < 0.001$. See also Figure S6A.

(E) Primary Schwann cells were transduced with a lentivirus expressing RXRγ or a GFP-expressing control virus. Expression of indicated genes was analyzed 72 hr after transduction by qRT-PCR. Results are shown as mean ratio versus control virus levels from three independent experiments. Error bars: SEM. $^{**}p < 0.01$, $^{***}p < 0.001$.

(F) Primary Schwann cells were transfected with luciferase constructs and transduced with a lentivirus expressing RXRγ or a GFP-expressing control virus. Three days later cells were assayed for firefly luciferase activity, and levels were normalized against Renilla luciferase activity. Error bars: SEM from three independent experiments. $^{*}p < 0.05$.

(G) Primary Schwann cells were first transfected with a pool of siRNAs against raptor, and 5 hr later transduced with a lentivirus expressing RXRγ or a GFP-expressing control virus, and expression of indicated genes was analyzed 72 hr later by qRT-PCR. Results are shown as mean ratio versus control virus levels from three independent experiments. Error bars: SEM. $^{*}p < 0.05$, $^{**}p < 0.01$. See Figure S6B for qRT-PCR results of knockdown of raptor and overexpression of RXRγ in this experiment.

## DISCUSSION

The Akt/mTOR pathway has been implicated as a major player controlling myelination (Norrmén and Suter, 2013). Indeed, genetic ablation of mTOR in Schwann cells results in hypomyelination (Sherman et al., 2012). However, neither the downstream effectors involved nor the individual roles of the two functionally distinct mTOR complexes are known. Here, we have deleted *raptor* and *rictor* in Schwann cells, individually or together, leading to consequent loss of mTORC1 and/or mTORC2 signaling. This experimental strategy allowed us to determine individual roles of the mTOR-containing complexes in Schwann cells during PNS myelination. Loss of mTORC2 signaling alone had no detectable impact on Schwann cell differentiation or myelin formation. In contrast, mTORC1 deficiency in Schwann cells, in both raptor and raptor/rictor mutants, led to profound changes in peripheral nerves. mTORC1-deficient nerves were considerably smaller compared to controls, despite only a slight decrease in the number of myelinated axons (possibly due to excessive numbers of axons still left in large unsorted bundles). Moreover, we found an absence of large caliber axons (above 6 μm) in mTORC1-deficient sciatic nerves of young adults. Because axons may require trophic support from overlaying Schwann cells (Nave, 2010), similar to recent demonstrations for oligodendrocytes and their associated axons (Morrison et al., 2013), mTORC1-deficient Schwann cells might not be able to provide sufficient support to allow normal axon growth. Our raptor-deficient model provides a promising entry point to elucidate the molecular nature of such support that has been proposed but has remained largely enigmatic.

Hypomyelination is a major hallmark of mTORC1-deficient nerves, a feature already evident at the start of myelination. Although myelin was able to grow slowly in raptor mutants during adulthood, myelin thickness did not fully recover, because significant hypomyelination was sustained in 1-year-old mice. In addition, we found a marked delay in myelination initiation, whereas mTORC1 deficiency did not affect differentiation of Schwann cells to the promyelinating state in major ways.

In the search for factors that are responsible for the defective myelination downstream of mTORC1, attenuation of translation has to be considered due to the hypophosphorylation of the mTORC1 downstream targets 4E-BP1 and S6K observed in mTORC1-deficient nerves. Although such contributions remain a valid option, we did not find major changes in protein levels of myelin proteins and myelin regulators in raptor mutants during active myelination. Instead, our results suggest that only MBP might be translationally regulated downstream of mTORC1, in line with recent findings in oligodendrocytes (Bercury et al., 2014; Lebrun-Julien et al., 2014). Moreover, we detected no hypomyelination in adult *S6K1/2* double-deficient mutant mice. Thus, we turned to regulation of lipid biogenesis as an attractive contributing target that might be critically regulated by mTORC1 during Schwann cell myelination. Indeed, we found strongly decreased signaling by SREBPs, the central regulators of lipid synthesis, in raptor mutant nerves. This finding was accompanied by altered lipid composition and decreased levels of FAs and cholesterol. In support of a functional link of these features to proper myelination, hypomyelinated nerves and decreased FA synthesis were also characteristic of mice lacking the SREBP regulator SCAP in Schwann cells (Verheijen et al., 2009). Moreover, similar to raptor mutants, SCAP mutants showed myelin growth in adulthood, likely due to external lipid uptake, as also suggested by increased levels of essential FAs present in raptor mutant nerves. However, the current knowledge of functional roles of lipids and their relative compositions in peripheral nerves is still fragmentary. Correct lipid levels are likely to be required for multiple essential regulatory processes in peripheral nerves, including Schwann cell signaling, differentiation, support of axons, trafficking of myelin proteins, myelin compaction, and establishing electrophysiological characteristics (Chrast et al., 2011). Thus, decreased lipogenesis and abnormal lipid composition in raptor mutants may not only contribute to reduced myelin growth, but also to the observed slowed NCV.

Mice lacking the SREBP-controlled squalene synthase in Schwann cells, and thus endogenous cholesterol synthesis, are affected by severe hypomyelination (Saher et al., 2009), consistent with functional contributions of decreased cholesterol levels to the hypomyelination in raptor mutants. Control of cholesterol in Schwann cells has been proposed as a major regulatory mechanism coordinating and balancing protein and lipid synthesis during myelination (Pertusa et al., 2007; Quintes et al., 2010; Saher et al., 2009). According to this hypothesis, low cholesterol levels lead to reduced transcription of genes encoding major myelin proteins as a potential safety mechanism guarding against deleterious effects of overexpression of myelin proteins. Furthermore, the persistence of Schwann cells at the promyelinating stage in raptor mutant nerves is consistent with results from mice with defective cholesterol synthesis and supports the notion that a threshold level of cholesterol is required for myelination initiation (Saher et al., 2009; Verheijen et al., 2009).

In addition to disturbed myelination initiation and progression, raptor mutants also showed persistence of immature, unsorted axon bundles. With time, the bundle size decreased, and later in adulthood Remak bundle-like structures appeared, albeit of abnormal morphology. Whether the defect is purely due to disturbances in radial sorting, or a combination of defective sorting and differentiation of specifically nonmyelinating Schwann cells, remains to be explored. However, as nerves from other mouse models with defective lipid synthesis do not, to our knowledge, display such a phenotype, the defect in Remak bundle maturation in mTORC1-deficient nerves is likely not due to decreased SREBP signaling, but rather due to disturbance of other pathway(s) downstream of mTORC1.

We show here that SREBPs are important downstream mediators of mTORC1 signaling in Schwann cells. Regulation of SREBPs by the mTOR pathway is known from other cell types, but the underlying mechanisms are not fully understood. We found downregulation of SREBP1c, but not of SREBP2, in both raptor mutant nerves and after raptor knockdown in Schwann cell cultures. Nevertheless, target genes of both SREBP1c and SREBP2 were strongly downregulated. Crosstalk between the SREBP1 and SREBP2 pathways could potentially explain these findings (Düvel et al., 2010). However, overexpression of RXRγ in Schwann cells led to increased levels of SREBP1c transcripts

and its target FASN, whereas the SREBP2 target IDI1 was not altered. Hence, these findings suggest minimal crosstalk between the SREBP1 and SREBP2 pathways in Schwann cells. Our data indicate that in Schwann cells, SREBP1c is transcriptionally controlled downstream of mTORC1, whereas SREBP2 is posttranslationally regulated. SREBPs can be regulated by mTORC1 at various levels, including induction of SREBP transcription, activation of ER-Golgi translocation, protein processing, posttranslational modifications, and protein stability (Bakan and Laplante, 2012). The mTORC1 substrate S6K has, in some settings, been suggested as mediator of SREBP regulation (Düvel et al., 2010; Owen et al., 2012), but we found no signs of hypomyelination in adult S6K1/2 mutant mice, rendering a role for S6K in myelin-related SREBP signaling unlikely. mTORC1-dependent SREBP regulation is also controlled by nuclear localization of lipin1 (Peterson et al., 2011). However, we found no striking changes in subcellular localization or expression levels of lipin1 in nerves of raptor mutants compared to controls. These results together point to substantial differences between Schwann cells and other cell types in terms of mTOR-dependent SREBP signaling, a notion further corroborated by our findings that mTORC2 deficiency in Schwann cells did not have a detectable impact on SREBP signaling, in contrast to reports from other cell types (Hagiwara et al., 2012; Yuan et al., 2012).

Our analysis of expression levels of factors involved in SREBP processing, including SCAP, INSIG1, INSIG2, and the proteases S1P and S2P, did not provide evidence for decreased processing of SREBPs in raptor mutant nerves. On the contrary, the transcript levels of INSIG1, a translocation inhibitor of the SCAP-SREBP complex from ER to Golgi, were even reduced, consistent with *Insig1* being a SREBP target gene and part of a feedback mechanism controlling SREBP levels (Gong et al., 2006). The parallel decrease of INSIG2 was unexpected, however, because it is not a SREBP target gene (Yabe et al., 2002). The promoter of *Insig2* carries a functional vitamin D response element (VDRE) that binds vitamin D receptor (VDR)-RXR heterodimers (Lee et al., 2005). Thus, it is conceivable that RXRγ (reduced in raptor mutants) is positively regulating INSIG2 expression in Schwann cells, similar to the SREBP-INSIG1 feedback loop.

Although SREBP1c regulates its own transcription via SRE binding sites in its promoter (Horton et al., 2003), and hence any defective process affecting SREBP1c activity may decrease SREBP1c transcription, the highly reduced transcript levels of SREBP1c in raptor mutants suggested potential involvements of additional regulating factors in Schwann cells downstream of mTORC1 signaling. Our search for such candidates revealed a striking downregulation of the retinoid X receptor RXRγ in raptor mutant nerves. This finding was of particular interest because loss of RXRγ in oligodendrocytes inhibits CNS remyelination by disturbing oligodendrocyte differentiation (Huang et al., 2011). In support of functional consequences of the reduced RXRγ levels in raptor mutant nerves, knockdown of RXRγ in cultured Schwann cells caused downregulation of SREBP1c and its target SCD1, but not of SREBP2 or its target IDI1. This mirrors the findings of raptor knockdown, with the exception of IDI1 expression, which was reduced both in raptor knockdown cells and in raptor mutant nerves, likely due to missing mTORC1-mediated post-transcriptional regulation of SREBP2 activity. Conversely, overexpression of RXRγ increased the levels of both SREBP1c and its target FASN, whereas SREBP2 and IDI1 remained unchanged. Moreover, luciferase reporter assays showed that RXRγ activates the SREBP1c promoter, but not the SREBP2 promoter, in cultured primary Schwann cells. Together, these results indicate that RXRγ regulates SREBP1c (but not SREBP2) expression in Schwann cells downstream of mTORC1. Upregulation of RXRγ expression, together with other RXR and RAR receptors, have been observed in Schwann cell-dorsal root ganglia neuron (SC-DRGN) cocultures upon induction of myelination (Latasa et al., 2010). Moreover, downregulation of RXRγ mRNA levels in both Schwann cells and SC-DRGN cocultures by the RXR ligand retinoic acid was concomitant with inhibition of myelination in SC-DRGN cocultures (Latasa and Cosgaya, 2011; Latasa et al., 2010). These data are consistent with our hypothesis that mTORC1 controls myelination through RXRγ-mediated SREBP1c regulation. The question remains, however, of how RXRγ is regulated by mTORC1. Retinoic-acid-dependent downregulation of RXRγ in Schwann cells is likely mediated via RAR receptors (Latasa and Cosgaya, 2011), and RARα was identified as a phosphoprotein downstream of mTOR in a screen for mTORC1 substrates (Yu et al., 2011). Thus, RAR phosphorylation downstream of mTORC1 might be required for its regulation of RXRγ. However, because no putative RAR binding elements were found in the *Rxrg* promoter, such a regulation is unlikely to be direct (Latasa and Cosgaya, 2011).

In conclusion, we show that mTOR signaling, specifically mediated by mTORC1, is a central regulator of PNS myelination, axonal growth, and lipid metabolism. Because dysregulation of the mTOR pathway has been implicated in hereditary peripheral neuropathies (Goebbels et al., 2012) and is likely to play important regulatory roles in neuropathies associated with metabolic disorders, our results also provide significant knowledge toward the understanding of the pathophysiology of these conditions.

## EXPERIMENTAL PROCEDURES

### Mice

Mutant mice were obtained by crossing mice with floxed alleles of *raptor* and/or *rictor* (Bentzinger et al., 2008; Polak et al., 2008) with mice expressing Cre under the *Dhh* promoter (Jaegle et al., 2003). Littermates lacking Cre were used as controls. Nerves from *S6K1*$^{-/-}$/*S6K2*$^{-/-}$ mice were a gift from Mario Pende (Pende et al., 2004). Animal experiments were approved by the Veterinary Office of the Canton of Zurich, Switzerland.

### Histology and Immunohistochemistry

Microscopy of sciatic nerves was performed as described (Pereira et al., 2010); see Supplemental Experimental Procedures for details, including antibodies used.

### Biochemistry

Western blotting and quantitative RT-PCR (qRT-PCR) were performed from epineurium-stripped sciatic nerves according to standard protocols; see Supplemental Experimental Procedures for details, including antibodies and primer sequences.

### Lentivirus Generation

To generate overexpression lentivirus, the coding region of mouse *Rxrg* (NM_009107.3) was cloned into a pCCLsin.PPT.hPGK.PRE lentiviral

backbone. The hPGK promoter was replaced by a 1.1 kb fragment of the rat P0 promoter (Messing et al., 1992). For virus production, HEK293T cells were transfected with viral constructs and packaging plasmids using Lipofectamine 2000 (Invitrogen).

### Cell-Culture Analyses

Primary rat Schwann cells (used in all experiments) were obtained as described (Jacob et al., 2008). For knockdown studies, cells were transfected with pools of two siRNAs for each target (ON-TARGET plus siRNA, Thermo Scientific) using DharmaFECT transfection reagent (Thermo Scientific). ON-TARGET plus nontargeting siRNA was used as control. Three days after transfection, cells were lysed with Qiazol lysis reagent and analyzed by qRT-PCR. For overexpression experiments, cells were transduced with RXRγ-overexpressing lentivirus or GFP-expressing control virus. Three days later, cells were analyzed using qRT-PCR. For luciferase assays, cells were transfected with a pGL3-Basic firefly luciferase vector containing the full-length rat SREBP1c promoter (1.5 kb) (Deng et al., 2002), a pGL2-Basic firefly luciferase vector containing the mouse SREBP2 promoter (−4316) (Shin and Osborne, 2003), or the corresponding vector backbones without the promoter sequences. A Renilla luciferase vector was used as an internal control. Five hours later, cells were transduced with RXRγ-overexpressing lentivirus or GFP-expressing control virus, and after 3 days cells were assayed for luciferase activity using Dual-Luciferase Reporter Assay System (Promega).

### Lipid Analysis

For lipid profiling, sciatic nerves from P60 mice were stripped from the epineurium, and lipids were extracted and analyzed using mass spectrometry as previously described (Lebrun-Julien et al., 2014). See Supplemental Experimental Procedures for details.

### Electrophysiology

NCV were measured in 4-month-old anesthetized mice as described (Bremer et al., 2010). Briefly, upon stimulation of the tibial nerve at the ankle ("distal") and of the sciatic nerve at the sciatic notch ("proximal"), compound muscle action potentials (CMAPs), measuring motor NCV, were recorded from the foot muscle. Motor NCV (mNCV) was calculated from the difference between distal and proximal latencies. Compound sensory nerve action potentials, measuring compound sensory NCV (csNCV), were recorded from the proximal sciatic nerve after stimulating the tibial nerve at the ankle, similarly as in the motor conduction studies.

### Statistical Analysis

Data are shown as mean ± SEM. Statistical significance was determined using a two-tailed Student's t test. Significance was set at $^{*}p < 0.05$, $^{**}p < 0.01$, and $^{***}p < 0.001$. *N* refers to the number of independent animals analyzed unless indicated differently.

## SUPPLEMENTAL INFORMATION

Supplemental Information includes Supplemental Experimental Procedures, six figures, and two tables and can be found with this article online at http://dx.doi.org/10.1016/j.celrep.2014.09.001.

## AUTHOR CONTRIBUTIONS

C.N. and U.S. designed research and wrote the paper; C.N. performed majority of research, with assistance from G.F., F.L.-J., and J.A.P.; M.T. and H.C.K. performed lipid analysis; V.R. designed and performed automated nerve quantifications; C.W. performed electrophysiology; A.L.F.v.D., A.B.S., and M.H.G.V. provided reagents and intellectual input; M.A.R. and M.N.H. contributed analytic tools. All authors read and commented the manuscript.

## ACKNOWLEDGMENTS

We thank Drs. Dies Meijer (University of Edinburgh) for *Dhh*-Cre mice, Mario Pende and Karim Nadra (INSERM, Paris) for samples of *S6K1*$^{-/-}$/*S6K2*$^{-/-}$ mutant mice, Werner Kovacs (ETH Zürich) for HMGCR and IDI1 antibodies, Thurl Harris (University of Virginia, Charlottesville) for lipin1 antibodies, Dies Meijer for Oct6 antibodies, Timothy Osborne (Sanford-Burnham Medical Research Institute, Orlando) for the SREBP2-pGL2 luciferase construct, and Marshall Elam and Xiong Deng (University of Tennessee Health Sciences Center, Memphis) for the SREBP1c-pGL3 luciferase construct. Members of U.S.'s lab, especially Deniz Gökbuget, are acknowledged for support and discussions, and Dr. Ned Mantei for critical reading of the manuscript. The electron microscopy data were collected at the Electron Microscopy Center, ETH Zürich. Research by C.N. was supported by a Marie Curie Intra-European Fellowship within the 7th European Community framework, Instrumentariumin Tiedesäätiö and Medicinska Understödsföreningen Liv och Hälsa. F.L.J. was supported by a Marie Curie International Incoming Fellowship within the 7th European Community framework and an ETH fellowship. U.S. is supported by the Swiss National Science Foundation.

Received: January 11, 2014
Revised: April 5, 2014
Accepted: August 28, 2014
Published: October 9, 2014

## REFERENCES

Bakan, I., and Laplante, M. (2012). Connecting mTORC1 signaling to SREBP-1 activation. Curr. Opin. Lipidol. *23*, 226–234.

Bentzinger, C.F., Romanino, K., Cloëtta, D., Lin, S., Mascarenhas, J.B., Oliveri, F., Xia, J., Casanova, E., Costa, C.F., Brink, M., et al. (2008). Skeletal muscle-specific ablation of raptor, but not of rictor, causes metabolic changes and results in muscle dystrophy. Cell Metab. *8*, 411–424.

Bercury, K.K., Dai, J., Sachs, H.H., Ahrendsen, J.T., Wood, T.L., and Macklin, W.B. (2014). Conditional ablation of raptor or rictor has differential impact on oligodendrocyte differentiation and CNS myelination. J. Neurosci. *34*, 4466–4480.

Bremer, J., Baumann, F., Tiberi, C., Wessig, C., Fischer, H., Schwarz, P., Steele, A.D., Toyka, K.V., Nave, K.A., Weis, J., and Aguzzi, A. (2010). Axonal prion protein is required for peripheral myelin maintenance. Nat. Neurosci. *13*, 310–318.

Chrast, R., Saher, G., Nave, K.A., and Verheijen, M.H. (2011). Lipid metabolism in myelinating glial cells: lessons from human inherited disorders and mouse models. J. Lipid Res. *52*, 419–434.

Cornu, M., Albert, V., and Hall, M.N. (2013). mTOR in aging, metabolism, and cancer. Curr. Opin. Genet. Dev. *23*, 53–62.

Cotter, L., Ozçelik, M., Jacob, C., Pereira, J.A., Locher, V., Baumann, R., Relvas, J.B., Suter, U., and Tricaud, N. (2010). Dlg1-PTEN interaction regulates myelin thickness to prevent damaging peripheral nerve overmyelination. Science *328*, 1415–1418.

Deng, X., Cagen, L.M., Wilcox, H.G., Park, E.A., Raghow, R., and Elam, M.B. (2002). Regulation of the rat SREBP-1c promoter in primary rat hepatocytes. Biochem. Biophys. Res. Commun. *290*, 256–262.

Düvel, K., Yecies, J.L., Menon, S., Raman, P., Lipovsky, A.I., Souza, A.L., Triantafellow, E., Ma, Q., Gorski, R., Cleaver, S., et al. (2010). Activation of a metabolic gene regulatory network downstream of mTOR complex 1. Mol. Cell *39*, 171–183.

Dyck P. and Thomas P.K., eds. (2005). Peripheral Neuropathy, Fourth Edition (Philadelphia: Saunders).

Efeyan, A., and Sabatini, D.M. (2010). mTOR and cancer: many loops in one pathway. Curr. Opin. Cell Biol. *22*, 169–176.

Flores, A.I., Narayanan, S.P., Morse, E.N., Shick, H.E., Yin, X., Kidd, G., Avila, R.L., Kirschner, D.A., and Macklin, W.B. (2008). Constitutively active Akt induces enhanced myelination in the CNS. J. Neurosci. *28*, 7174–7183.

Garbay, B., Boiron-Sargueil, F., Shy, M., Chbihi, T., Jiang, H., Kamholz, J., and Cassagne, C. (1998). Regulation of oleoyl-CoA synthesis in the peripheral

nervous system: demonstration of a link with myelin synthesis. J. Neurochem. *71*, 1719–1726.

Garbay, B., Heape, A.M., Sargueil, F., and Cassagne, C. (2000). Myelin synthesis in the peripheral nervous system. Prog. Neurobiol. *61*, 267–304.

Goebbels, S., Oltrogge, J.H., Wolfer, S., Wieser, G.L., Nientiedt, T., Pieper, A., Ruhwedel, T., Groszer, M., Sereda, M.W., and Nave, K.A. (2012). Genetic disruption of Pten in a novel mouse model of tomaculous neuropathy. EMBO Mol. Med. *4*, 486–499.

Gong, Y., Lee, J.N., Lee, P.C., Goldstein, J.L., Brown, M.S., and Ye, J. (2006). Sterol-regulated ubiquitination and degradation of Insig-1 creates a convergent mechanism for feedback control of cholesterol synthesis and uptake. Cell Metab. *3*, 15–24.

Hagiwara, A., Cornu, M., Cybulski, N., Polak, P., Betz, C., Trapani, F., Terracciano, L., Heim, M.H., Rüegg, M.A., and Hall, M.N. (2012). Hepatic mTORC2 activates glycolysis and lipogenesis through Akt, glucokinase, and SREBP1c. Cell Metab. *15*, 725–738.

Horton, J.D., Shah, N.A., Warrington, J.A., Anderson, N.N., Park, S.W., Brown, M.S., and Goldstein, J.L. (2003). Combined analysis of oligonucleotide microarray data from transgenic and knockout mice identifies direct SREBP target genes. Proc. Natl. Acad. Sci. USA *100*, 12027–12032.

Huang, J.K., Jarjour, A.A., Nait Oumesmar, B., Kerninon, C., Williams, A., Krezel, W., Kagechika, H., Bauer, J., Zhao, C., Baron-Van Evercooren, A., et al. (2011). Retinoid X receptor gamma signaling accelerates CNS remyelination. Nat. Neurosci. *14*, 45–53.

Jacob, C., Grabner, H., Atanasoski, S., and Suter, U. (2008). Expression and localization of Ski determine cell type-specific TGFbeta signaling effects on the cell cycle. J. Cell Biol. *182*, 519–530.

Jaegle, M., Ghazvini, M., Mandemakers, W., Piirsoo, M., Driegen, S., Levavasseur, F., Raghoenath, S., Grosveld, F., and Meijer, D. (2003). The POU proteins Brn-2 and Oct-6 share important functions in Schwann cell development. Genes Dev. *17*, 1380–1391.

Jessen, K.R., and Mirsky, R. (2005). The origin and development of glial cells in peripheral nerves. Nat. Rev. Neurosci. *6*, 671–682.

Laplante, M., and Sabatini, D.M. (2012). mTOR signaling in growth control and disease. Cell *149*, 274–293.

Latasa, M.J., and Cosgaya, J.M. (2011). Regulation of retinoid receptors by retinoic acid and axonal contact in Schwann cells. PLoS ONE *6*, e17023.

Latasa, M.J., Ituero, M., Moran-Gonzalez, A., Aranda, A., and Cosgaya, J.M. (2010). Retinoic acid regulates myelin formation in the peripheral nervous system. Glia *58*, 1451–1464.

Lebrun-Julien, F., Bachmann, L., Norrmén, C., Trötzmüller, M., Köfeler, H., Rüegg, M.A., Hall, M.N., and Suter, U. (2014). Balanced mTORC1 activity in oligodendrocytes is required for accurate CNS myelination. J. Neurosci. *34*, 8432–8448.

Lee, S., Lee, D.K., Choi, E., and Lee, J.W. (2005). Identification of a functional vitamin D response element in the murine Insig-2 promoter and its potential role in the differentiation of 3T3-L1 preadipocytes. Mol. Endocrinol. *19*, 399–408.

Messing, A., Behringer, R.R., Hammang, J.P., Palmiter, R.D., Brinster, R.L., and Lemke, G. (1992). P0 promoter directs expression of reporter and toxin genes to Schwann cells of transgenic mice. Neuron *8*, 507–520.

Morrison, B.M., Lee, Y., and Rothstein, J.D. (2013). Oligodendroglia: metabolic supporters of axons. Trends Cell Biol. *23*, 644–651.

Nave, K.A. (2010). Myelination and support of axonal integrity by glia. Nature *468*, 244–252.

Newbern, J., and Birchmeier, C. (2010). Nrg1/ErbB signaling networks in Schwann cell development and myelination. Semin. Cell Dev. Biol. *21*, 922–928.

Norrmén, C., and Suter, U. (2013). Akt/mTOR signalling in myelination. Biochem. Soc. Trans. *41*, 944–950.

Owen, J.L., Zhang, Y., Bae, S.H., Farooqi, M.S., Liang, G., Hammer, R.E., Goldstein, J.L., and Brown, M.S. (2012). Insulin stimulation of SREBP-1c processing in transgenic rat hepatocytes requires p70 S6-kinase. Proc. Natl. Acad. Sci. USA *109*, 16184–16189.

Pellegatta, M., De Arcangelis, A., D'Urso, A., Nodari, A., Zambroni, D., Ghidinelli, M., Matafora, V., Williamson, C., Georges-Labouesse, E., Kreidberg, J., et al. (2013). $\alpha6\beta1$ and $\alpha7\beta1$ integrins are required in Schwann cells to sort axons. J. Neurosci. *33*, 17995–18007.

Pende, M., Um, S.H., Mieulet, V., Sticker, M., Goss, V.L., Mestan, J., Mueller, M., Fumagalli, S., Kozma, S.C., and Thomas, G. (2004). S6K1(-/-)/S6K2(-/-) mice exhibit perinatal lethality and rapamycin-sensitive 5′-terminal oligopyrimidine mRNA translation and reveal a mitogen-activated protein kinase-dependent S6 kinase pathway. Mol. Cell. Biol. *24*, 3112–3124.

Pereira, J.A., Benninger, Y., Baumann, R., Gonçalves, A.F., Ozçelik, M., Thurnherr, T., Tricaud, N., Meijer, D., Fässler, R., Suter, U., and Relvas, J.B. (2009). Integrin-linked kinase is required for radial sorting of axons and Schwann cell remyelination in the peripheral nervous system. J. Cell Biol. *185*, 147–161.

Pereira, J.A., Baumann, R., Norrmén, C., Somandin, C., Miehe, M., Jacob, C., Lühmann, T., Hall-Bozic, H., Mantei, N., Meijer, D., and Suter, U. (2010). Dicer in Schwann cells is required for myelination and axonal integrity. J. Neurosci. *30*, 6763–6775.

Pereira, J.A., Lebrun-Julien, F., and Suter, U. (2012). Molecular mechanisms regulating myelination in the peripheral nervous system. Trends Neurosci. *35*, 123–134.

Pertusa, M., Morenilla-Palao, C., Carteron, C., Viana, F., and Cabedo, H. (2007). Transcriptional control of cholesterol biosynthesis in Schwann cells by axonal neuregulin 1. J. Biol. Chem. *282*, 28768–28778.

Peterson, T.R., Sengupta, S.S., Harris, T.E., Carmack, A.E., Kang, S.A., Balderas, E., Guertin, D.A., Madden, K.L., Carpenter, A.E., Finck, B.N., and Sabatini, D.M. (2011). mTOR complex 1 regulates lipin 1 localization to control the SREBP pathway. Cell *146*, 408–420.

Polak, P., Cybulski, N., Feige, J.N., Auwerx, J., Rüegg, M.A., and Hall, M.N. (2008). Adipose-specific knockout of raptor results in lean mice with enhanced mitochondrial respiration. Cell Metab. *8*, 399–410.

Porstmann, T., Santos, C.R., Griffiths, B., Cully, M., Wu, M., Leevers, S., Griffiths, J.R., Chung, Y.L., and Schulze, A. (2008). SREBP activity is regulated by mTORC1 and contributes to Akt-dependent cell growth. Cell Metab. *8*, 224–236.

Quintes, S., Goebbels, S., Saher, G., Schwab, M.H., and Nave, K.A. (2010). Neuron-glia signaling and the protection of axon function by Schwann cells. J. Peripher. Nerv. Syst. *15*, 10–16.

Repa, J.J., Liang, G., Ou, J., Bashmakov, Y., Lobaccaro, J.-M.A., Shimomura, I., Shan, B., Brown, M.S., Goldstein, J.L., and Mangelsdorf, D.J. (2000). Regulation of mouse sterol regulatory element-binding protein-1c gene (SREBP-1c) by oxysterol receptors, LXRalpha and LXRbeta. Genes Dev. *14*, 2819–2830.

Saher, G., Quintes, S., Möbius, W., Wehr, M.C., Krämer-Albers, E.M., Brügger, B., and Nave, K.A. (2009). Cholesterol regulates the endoplasmic reticulum exit of the major membrane protein P0 required for peripheral myelin compaction. J. Neurosci. *29*, 6094–6104.

Shao, W., and Espenshade, P.J. (2012). Expanding roles for SREBP in metabolism. Cell Metab. *16*, 414–419.

Sherman, D.L., Krols, M., Wu, L.M., Grove, M., Nave, K.A., Gangloff, Y.G., and Brophy, P.J. (2012). Arrest of myelination and reduced axon growth when Schwann cells lack mTOR. J. Neurosci. *32*, 1817–1825.

Shin, D.J., and Osborne, T.F. (2003). Thyroid hormone regulation and cholesterol metabolism are connected through Sterol Regulatory Element-Binding Protein-2 (SREBP-2). J. Biol. Chem. *278*, 34114–34118.

Verheijen, M.H., Camargo, N., Verdier, V., Nadra, K., de Preux Charles, A.S., Médard, J.J., Luoma, A., Crowther, M., Inouye, H., Shimano, H., et al. (2009). SCAP is required for timely and proper myelin membrane synthesis. Proc. Natl. Acad. Sci. USA *106*, 21383–21388.

Webster, H.D. (1971). The geometry of peripheral myelin sheaths during their formation and growth in rat sciatic nerves. J. Cell Biol. *48*, 348–367.

Yabe, D., Brown, M.S., and Goldstein, J.L. (2002). Insig-2, a second endoplasmic reticulum protein that binds SCAP and blocks export of sterol regulatory element-binding proteins. Proc. Natl. Acad. Sci. USA *99*, 12753–12758.

Yu, Y., Yoon, S.O., Poulogiannis, G., Yang, Q., Ma, X.M., Villén, J., Kubica, N., Hoffman, G.R., Cantley, L.C., Gygi, S.P., and Blenis, J. (2011). Phosphoproteomic analysis identifies Grb10 as an mTORC1 substrate that negatively regulates insulin signaling. Science *332*, 1322–1326.

Yuan, M., Pino, E., Wu, L., Kacergis, M., and Soukas, A.A. (2012). Identification of Akt-independent regulation of hepatic lipogenesis by mammalian target of rapamycin (mTOR) complex 2. J. Biol. Chem. *287*, 29579–29588.